Environmental Science & Technology

Article

pubs.acs.org/est

Formaldehyde (HCHO) As a Hazardous Air Pollutant: Mapping Surface Air Concentrations from Satellite and Inferring Cancer Risks in the United States

Lei Zhu,[*,†] Daniel J. Jacob,[†,‡] Frank N. Keutsch,[†,§] Loretta J. Mickley,[†] Richard Scheffe,[∥] Madeleine Strum,[∥] Gonzalo González Abad,[⊥] Kelly Chance,[⊥] Kai Yang,[#] Bernhard Rappenglück,[▽] Dylan B. Millet,[○] Munkhbayar Baasandorj,[○,¶] Lyatt Jaeglé,[◆] and Viral Shah[◆]

[†]John A. Paulson School of Engineering and Applied Sciences, Harvard University, Cambridge, Massachusetts 02138, United States

[‡]Department of Earth and Planetary Sciences, Harvard University, Cambridge, Massachusetts 02138, United States

[§]Department of Chemistry and Chemical Biology, Harvard University, Cambridge, Massachusetts 02138, United States

[∥]U.S. Environmental Protection Agency, Durham, North Carolina 27711, United States

[⊥]Harvard-Smithsonian Center for Astrophysics, Cambridge, Massachusetts 02138, United States

[#]Department of Atmospheric and Oceanic Science, University of Maryland College Park, College Park, Maryland 20740, United States

[▽]Department of Earth and Atmospheric Sciences, University of Houston, Houston, Texas 77204, United States

[○]Department of Soil, Water, and Climate, University of Minnesota, Minneapolis−Saint Paul, Minnesota 55108, United States

[◆]Department of Atmospheric Sciences, University of Washington, Seattle, Washington 98105, United States

ABSTRACT: Formaldehyde (HCHO) is the most important carcinogen in outdoor air among the 187 hazardous air pollutants (HAPs) identified by the U.S. Environmental Protection Agency (EPA), not including ozone and particulate matter. However, surface observations of HCHO are sparse and the EPA monitoring network could be prone to positive interferences. Here we use 2005−2016 summertime HCHO column data from the OMI satellite instrument, validated with high-quality aircraft data and oversampled on a 5 × 5 km^2 grid, to map surface air HCHO concentrations across the contiguous U.S. OMI-derived summertime HCHO values are converted to annual averages using the GEOS-Chem chemical transport model. Results are in good agreement with high-quality summertime observations from urban sites (−2% bias, r = 0.95) but a factor of 1.9 lower than annual means from the EPA network. We thus estimate that up to 6600−12 500 people in the U.S. will develop cancer over their lifetimes by exposure to outdoor HCHO. The main HCHO source in the U.S. is atmospheric oxidation of biogenic isoprene, but the corresponding HCHO yield decreases as the concentration of nitrogen oxides ($NO_x \equiv NO + NO_2$) decreases. A GEOS-Chem sensitivity simulation indicates that HCHO levels would decrease by 20−30% in the absence of U.S. anthropogenic NO_x emissions. Thus, NO_x emission controls to improve ozone air quality have a significant cobenefit in reducing HCHO-related cancer risks.

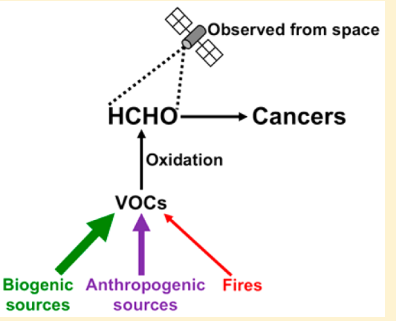

INTRODUCTION

Formaldehyde (HCHO) in outdoor air is a known carcinogen. Exposure to a mean HCHO concentration of 1 μg m^{-3} (about 0.7 ppb at STP) over one's lifetime will cause up to 13 people in a million to develop lung and nasopharyngeal cancer according to the U.S. Environmental Protection Agency (EPA).[1] HCHO is one of 187 hazardous air pollutants (HAPs) identified by the EPA[1] to cause cancer or other serious health impacts in ambient outside air. It is by far the most important HAP in terms of health risks, accounting for over 50% of the total HAPs-related cancer risks in the U.S.[2] The second most important HAP is benzene (~10%). Unlike most other HAPs, HCHO is not mainly associated with local anthropogenic hotspots but instead is widely present across the U.S. as a product of the oxidation of volatile organic compounds (VOCs) including in particular biogenic isoprene.[3] The HAPs sampling network in the U.S. provides information about human health exposure near the monitor location but it is limited to urban/industrial sites.[2] Here we use 12 years of HCHO observations from the OMI satellite instrument[4] with 5 × 5 km^2 spatial resolution enabled by an oversampling technique[5] to map HCHO surface air concentrations over the contiguous U.S. and infer cancer risks on a national scale.

EPA reports HCHO as an ambient air toxic using data from 300−400 sites operated by states, local agencies, and tribes

Received: March 14, 2017
Revised: April 25, 2017
Accepted: April 25, 2017
Published: April 25, 2017

DOI: 10.1021/acs.est.7b01356
Environ. Sci. Technol. XXXX, XXX, XXX−XXX

(SLTs network), including ~50 national air toxics trends sites (NATTS network). HCHO is collected by 2,4-dinitrophenylhydrazine (DNPH) coated cartridges and then analyzed by high-performance liquid chromatography (HPLC), known as the EPA compendium method TO-11A.[6] HCHO measured using this method has potential interferences by ozone[7] and NO_2.[8,9] High-quality HCHO measurements in surface air are available only from occasional field campaigns.[10−13] Satellites provide a continuously operating high spatial resolution data set. HCHO satellite data over the U.S. were recently validated using aircraft observations.[14] Although satellites only measure total HCHO columns (molecules per cm^2 of surface), the bulk of that column is in the boundary layer[14−16] and surface concentrations can therefore be inferred.

HCHO columns have been observed continuously from space since GOME[17] (1996−2003) and SCIAMACHY[18] (2003−2012). Observations are presently available from OMI[4,19] (2004−), GOME2A[20] (2006−), OMPS[21,22] (2011−) and GOME2B[19] (2012−) with better data quality during summertime when signals are stronger. These satellite sensors scan the whole earth every 1−2 days, OMI provides the most suitable data for HCHO mapping due to its daily global coverage, long data record, and fine pixel resolution (13 × 24 km^2 at nadir). Its spatial resolution can be further refined by oversampling, as described below.

MATERIALS AND METHODS

EPA Surface HCHO Observations. We obtain surface HCHO observations from the EPA SLTs network, available at https://www.epa.gov/outdoor-air-quality-data. EPA SLTs sites report 24 h average HCHO concentrations every 6 days. Here we select sites with full yearly coverage (at least 12 samples per quarter) for at least 9 years of the 2005−2016 period. 48 SLTs sites meet the above criteria and their locations are shown in the top panel of Figure 1. Also shown in Figure 1 are monthly mean surface HCHO concentrations averaged over those 48 sites. Surface HCHO peaks during summertime and this likely reflects higher biogenic VOC emissions.[23]

OMI Observations. OMI is a UV/vis nadir solar backscatter spectrometer launched in 2004 on the Aura satellite in a polar sun-synchronous orbit.[24] It observes the whole globe daily at 13:30 local time (LT). We use OMI HCHO Version 2.0 (Collection 3) retrievals from the Smithsonian Astrophysical Observatory (OMI-SAO),[4] available at http://disc.sci.gsfc.nasa.gov/Aura/data-holdings/OMI/omhcho_v003.shtml. The data archive extends from 2005 to present. We select data for June−August 2005−2016 that (1) pass all the fitting and statistical quality checks (MainDataQualityFlag = 0), (2) have cloud fraction less than 0.3 and solar zenith angle less than 60°, and (3) are not affected by the instrumental "row anomaly" (http://projects.knmi.nl/omi/research/product/rowanomaly-background). The single-scene precision is 1 × 10^{16} molecules cm^{-2},[4] which corresponds to about 2 ppb in a 2 km deep well-mixed boundary layer. The precision can be improved by multiscene averaging.[25,26] We only use the summertime data when HCHO columns are highest and detectable from space. HCHO columns in winter are generally below the detection limit due to (1) low biogenic VOC emissions, and (2) low OH concentrations delaying the oxidation of anthropogenic VOCs to HCHO and thus spatially smearing the HCHO signal.[5,23]

Zhu et al.[14] validated the OMI-SAO product with high-quality HCHO aircraft measurements from the SEAC^{4}RS flight campaign[27] over the Southeast U.S. in August−September 2013. Aircraft measurements during SEAC^{4}RS were made in situ from 0.3 to 12 km altitude by two independent laser instruments: CAMS[28] and ISAF.[29] The two instruments were extremely consistent throughout the campaign with correlation coefficient of 0.99 for 1 min averages. Mean HCHO measured by ISAF was 10% higher than CAMS. The horizontal patterns from the satellite retrievals were highly correlated with the aircraft and consistent with a dominant source from biogenic isoprene.[16] However, the retrievals were biased low by 37% relative to the CAMS aircraft data, which Zhu et al.[14] attributed to errors in spectral fitting and in assumed surface reflectivity. Independent aircraft validation[30,31] of OMI-SAO retrievals finds similar mean biases: −51% for the DC-3 campaign over the central U.S. in May−June, 2012, and −42% for the DISCOVER-AQ campaign including deployments in Baltimore (July 2007), central California (January 2013) and Houston (August 2013). There is no evident spatial or temporal pattern in the biases, implying that they may be removed by applying uniform correction factors.[14] Here we apply a uniform correction factor of 1.59 to the OMI-SAO retrieval to correct the −37% bias relative to CAMS in SEAC^{4}RS.

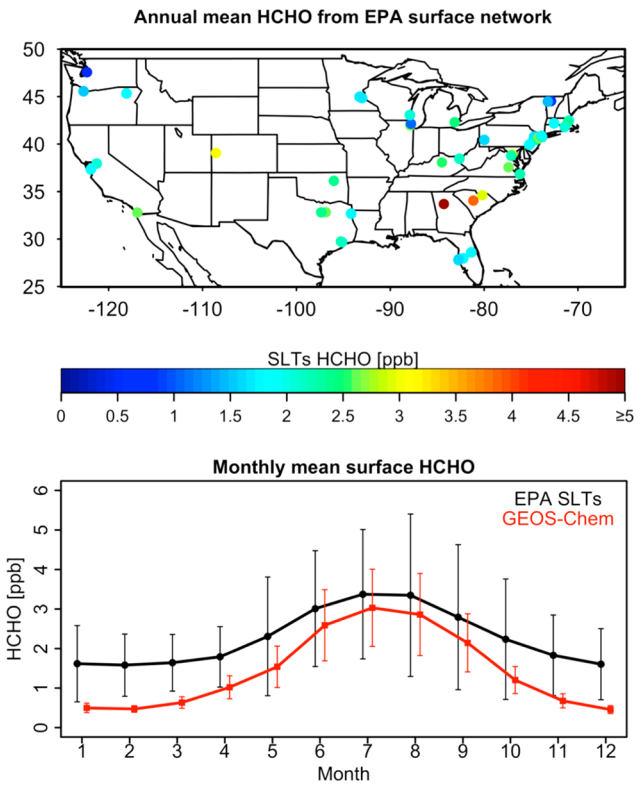

Figure 1. Annual and monthly mean 2005−2016 HCHO concentrations from the EPA surface network (SLTs). Top panel shows the network site locations and the annual mean data. Only sites with at least 9 years of complete data for the 2005−2016 period are used (see text for details). Bottom panel shows monthly mean HCHO concentrations spatially averaged across those sites (black, with standard deviations shown as vertical bars). GEOS-Chem model values sampled at the same sites are shown in red.

Oversampling Method. Relating concentrations to population exposure requires the highest spatial resolution possible. Temporal resolution is less critical since the HCHO cancer risk is based on a lifetime-averaged exposure. Here we oversample the OMI HCHO data to increase spatial resolution to 5 × 5 km^2 through temporal averaging. Oversampling takes

DOI: 10.1021/acs.est.7b01356
Environ. Sci. Technol. XXXX, XXX, XXX−XXX

advantage of shifting pixel locations and sizes in day-to-day observations[32,33] to achieve a spatial resolution finer than pixel size as a temporal average. Oversampling of OMI observations to achieve an effective spatial resolution of a few km has been used previously on urban/regional scales for HCHO,[5] SO_2,[33−36] and NO_2.[33,36] The common assumption in all these studies has been to view individual satellite observations as uniformly representative of a circle around the pixel center, with the circle radius optimized to balance smoothing and noise. This approach is somewhat arbitrary and computationally demanding.

Here we developed an improved and faster oversampling method enabling application over the entire contiguous U.S. Consider a satellite pixel p with HCHO column $\Omega(p)$. The overlap area between the pixel p and oversampling grid cell i is $A(p,i)$. Grid cell i collects $N(i)$ overlapping satellite pixel data points over the oversampling period, from which an average column for that grid cell is calculated. We assume that the averaging weight for each individual satellite observation is proportional to the ratio of the overlap area $A(p,i)$ to the pixel area $S(p)$ and inversely proportional to the absolute error standard deviation $\sigma(p)$ of that observation as reported in the OMI-SAO product. $S(p)$ varies by a factor of 10 from ∼300 km^2 at nadir to ∼3000 km^2 at the outermost swath-angle.[24,37] $\sigma(p)$ can vary by a factor of 6 from 0.2×10^{16} molecules cm^{-2} for background conditions to 1.2×10^{16} molecules cm^{-2} in high-concentration regions.[4] The area- and error-weighted average column for grid cell i is then derived as

$$\bar{\Omega}(i) = \frac{\sum_{p=1}^{N(i)} \frac{A(p,i)}{S(p)\sigma(p)} \Omega(p)}{\sum_{p=1}^{N(i)} \frac{A(p,i)}{S(p)\sigma(p)}} \quad (1)$$

Besides being computationally fast, this method has the advantage that it fully uses and appropriately weighs the information from all individual satellite observations.

We applied our oversampling method to the OMI observations to produce a 12-year (June−August 2005−2016) summer average map of HCHO columns with 0.05° × 0.05° (≈ 5 × 5 km^2) grid resolution. Figure 2 shows the result. Values are highest over the Southeast U.S. and are due to oxidation of biogenic isoprene.[3,38] The Southeast data were previously validated with the SEAC^{4}RS aircraft observations described above. The HCHO column peaks in the urban areas of Atlanta, Birmingham, and Houston, which could reflect industrial and vehicle sources.[5,25,39−41] However, these peaks are relatively modest on top of the biogenic enhancement. More detailed inspection of the Atlanta maximum (bottom panel of Figure 2) suggests a source from ring road traffic. Summertime HCHO hotspots in the western U.S. are mostly due to fires as biogenic emissions in that part of the country are generally lower than in the eastern U.S. Satellite retrievals of HCHO columns in fire plumes are highly uncertain because of strong sensitivity to plume rise and to light extinction by the smoke particles.[42]

Deriving Annual Mean Surface HCHO Concentrations. We use the summer mean 0.05° × 0.05° satellite data for HCHO columns in combination with eq 2 to derive the annual mean surface concentrations required for cancer risk assessments:

$$\bar{C}(i) = \bar{\Omega}(i)\gamma_1(i)\gamma_2(i)\gamma_3(i) \quad (2)$$

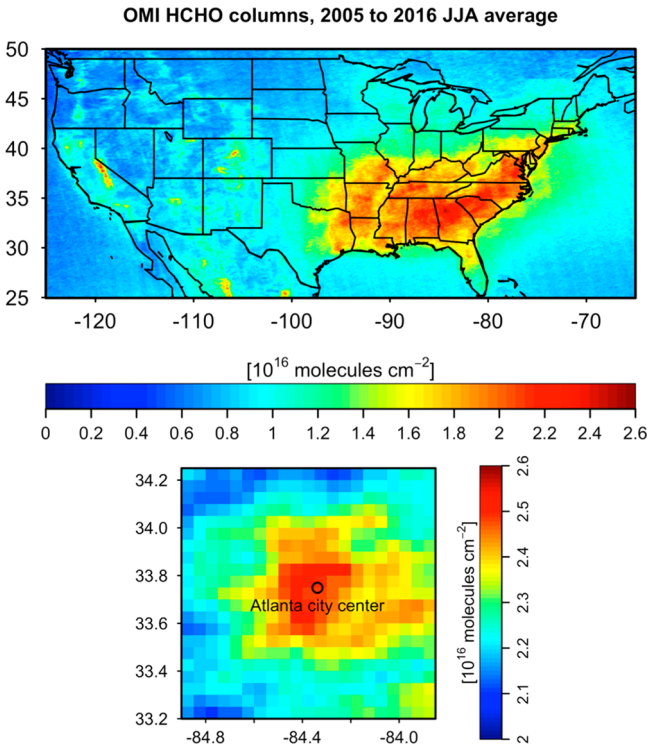

Figure 2. Mean OMI HCHO columns over the contiguous U.S. for June−August 2005−2016 with oversampling on a 0.05° × 0.05° (≈ 5 × 5 km^2) grid. The bottom panel zooms in on the ∼100 × 100 km^2 Atlanta area with a different scale. The black circle indicates the Atlanta city center.

Here $\bar{C}(i)$ is the annual mean surface air concentration in 0.05° × 0.05° grid cell i, $\bar{\Omega}(i)$ is the summer mean oversampled OMI column in that grid cell (Figure 2), $\gamma_1(i)$ is the ratio of midday surface air to column concentrations in summer, $\gamma_2(i)$ is the ratio of 24-h average to midday concentrations in summer, and $\gamma_3(i)$ is the ratio of annual to summer mean concentrations. We use a GEOS-Chem chemical transport model to infer γ_1 and γ_3, and surface observations to infer γ_2. GEOS-Chem is driven by GEOS-5 assimilated meteorological fields[43] produced at 0.25° × 0.3125° resolution by the NASA Global Modeling and Assimilation Office (GMAO). It is applied here in a 2010 simulation with 2° × 2.5° horizontal resolution, and results for γ_1 and γ_3 are assumed to apply to the 2005−2016 period (interannual variability in the model is small).

GEOS-Chem has been used previously in several studies to simulate HCHO over the U.S. including comparisons to satellite and in situ observations.[3,16,44,45] Zhu et al.[14] and Miller et al.[45] find that GEOS-Chem provides an unbiased simulation of SEAC^{4}RS and SENEX aircraft observations in the boundary layer over the Southeast U.S. in summer, including horizontal patterns and mean vertical profiles. GEOS-Chem is biased by −32% compared to WINTER aircraft observations[46] below 300 m over the Northeast U.S. in winter. Our own work shows a wintertime low bias in comparison with EPA SLTs sites (Figure 1 bottom panel), resulting in a mean −37% bias on an annual mean basis. As pointed out above, there may be positive interferences in the EPA data. In addition, the EPA sites are located near urban/industrial sources that the model may not be able to resolve particularly under wintertime stratified conditions. We will consider this bias in the error analysis.

DOI: 10.1021/acs.est.7b01356
Environ. Sci. Technol. XXXX, XXX, XXX−XXX

In order to convert HCHO columns to surface concentrations (scaling factor γ_1), we sample daily surface HCHO concentrations and total columns from the June−August model output at the OMI overpass time (13:00−14:00 LT; midday here and elsewhere). Figure 3 shows the resulting summer

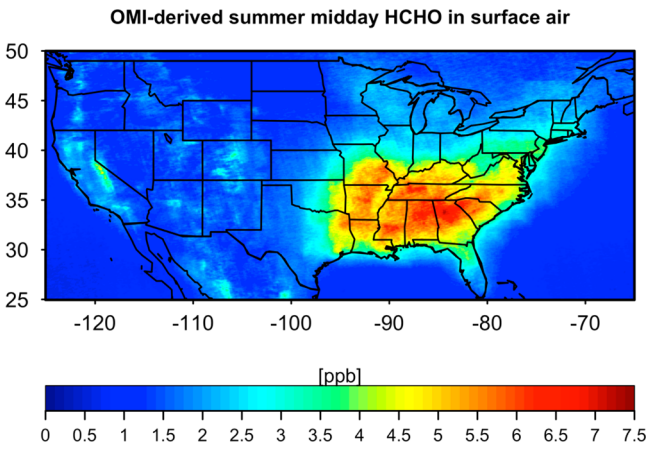

Figure 3. OMI-derived summer midday HCHO concentrations in surface air. Values are 2005−2016 averages for June−August at 13:00−14:00 local time.

midday mean surface concentrations. The spatial patterns in the OMI data are retained because the GEOS-Chem scaling factors are fairly uniform. Figure 4 compares this product with local

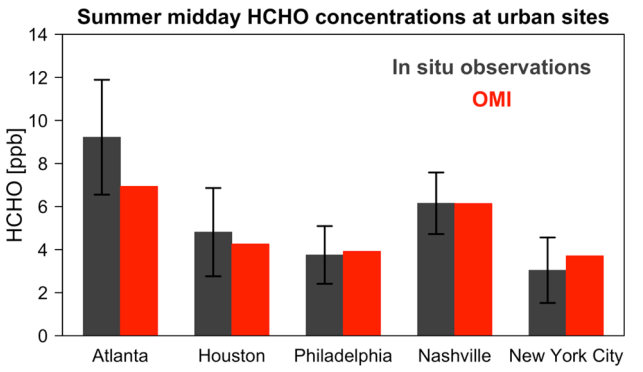

Figure 4. Summer mean midday HCHO concentrations at urban sites. OMI-derived values for 2005−2016 are compared to local measurements in different years. Measurements for Houston are from the Moody Tower in August 2006 and 2010 (B. Rappenglück, unpublished data). Measurements for New York City are from Lin et al.[11] Measurements for Atlanta, Philadelphia, and Nashville are from Dasgupta et al.[47] Error bars represent ±1 standard deviation in the measurements.

measurements from summertime research field campaigns at several urban sites[11,47] and in Houston (B. Rappenglück, unpublished data). There is good agreement with no significant bias averaged across all sites (−2.0 ± 18%), and successful simulation of variability between cities (r = 0.95). This provides support for the uniform correction factor of 1.59 applied to the OMI-SAO retrieval. A larger correction factor would result in bias in the simulation of the data in Figure 4.

To convert midday to 24 h averaged surface air HCHO concentrations (scaling factor γ_2), we use ground-site HCHO measurements from the three field campaigns where such high-quality data have been reported to our knowledge: (1) CalNex (May−June 2010, Pasadena, California), (2) SOAS (June−July 2013, Brent, Alabama), and (3) SLAQRS (August−September 2013, East St. Louis, Illinois).[10,12,13] Figure 5 shows the diurnal

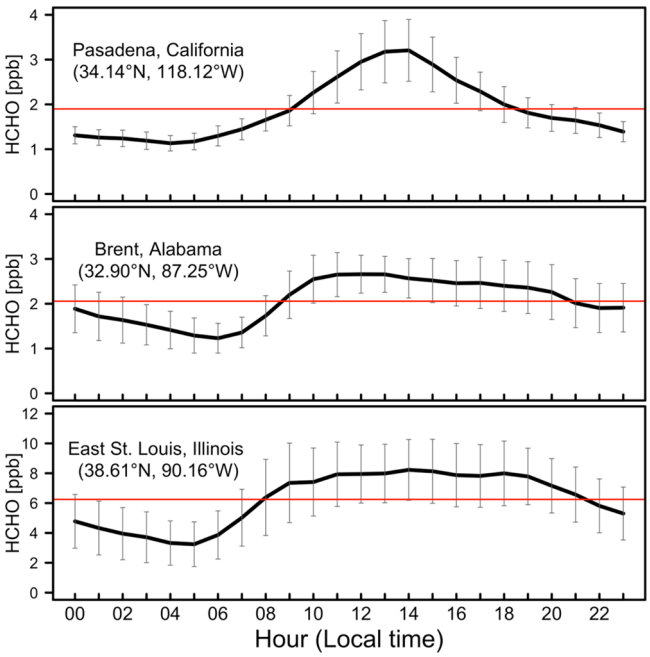

Figure 5. Diurnal variation of summertime HCHO concentrations in surface air. Observations are from three field campaigns including CalNex (May−June 2010)[10] in Pasadena, California; SOAS (June−July 2013)[13] in Brent, Alabama; and SLAQRS (August−September 2013)[12] in East St. Louis, Illinois. Error bars are standard deviations in the hourly averaged data. Red lines are 24 h averages.

variations in HCHO concentrations measured at those three sites. Pasadena and East St. Louis are urban, Brent is rural. HCHO is depleted during the night because of dry deposition.[48] The 24 h average to midday value ratio is consistent among the three sites: 0.64 (Pasadena), 0.77 (Brent), 0.79 (East St. Louis). It is not clear that these differences reflect geographical specificity, therefore we apply a single scaling factor γ_2 = 0.73 throughout the U.S. to convert midday to 24 h average summer concentrations.

Finally, we use GEOS-Chem to convert these summertime 24 h averages to annual 24 h averages (scaling factor γ_3; Figure 6). Surface HCHO concentrations in GEOS-Chem have strong

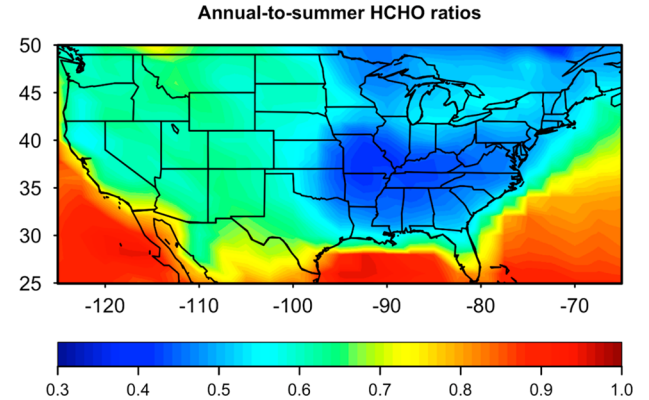

Figure 6. Ratios of annual to summer (JJA) mean HCHO concentrations in surface air. Values are from the GEOS-Chem model.

DOI: 10.1021/acs.est.7b01356
Environ. Sci. Technol. XXXX, XXX, XXX−XXX

seasonal variations driven mostly by biogenic emissions, with annual to summertime average ratios of 0.4−0.5 in the Southeast U.S. and 0.6−0.7 in the West. GEOS-Chem may underestimate wintertime concentrations, as pointed out above, in which case γ_3 would be biased low. This will be accounted for in error analysis of the results.

Estimating Cancer Risks. EPA uses the inhalation unit risk estimate (URE) to quantify the cancer risks of HCHO and other HAPs.[1] The URE represents the upper bound for the increased cancer risk from inhalation exposure to an air concentration of 1 μg m^{-3} over an individual's lifetime. Based on the upper confidence limit of the fitted dose−response curve, the inhalation URE for HCHO is estimated to be 1.3 × 10^{-5} (μg m^{-3})$^{-1}$ by the Agency's Integrated Risk Information System (IRIS).[1,2] This means that individuals exposed to a mean HCHO concentration of 1 μg m^{-3} (about 0.7 ppb) have a chance of up to 13 in a million to develop cancer over their lifetime from this HCHO exposure. Risk is assumed to increase linearly with HCHO concentration.

RESULTS AND DISCUSSION

Annual Mean Surface HCHO Concentrations. Figure 7 shows the annual mean HCHO concentrations in surface air across the U.S. as derived from eq 2. We find that these OMI-derived values are on average 47% lower than at the EPA SLTs sites of Figure 1. As discussed above, the difference could be due to (1) excessive GEOS-Chem seasonal scaling in converting OMI summer to annual means, (2) positive artifacts in the EPA data, (3) local influences in the EPA data not resolved by OMI. We superimpose on Figure 7 the EPA 2005−2016 data (same data as Figure 1), decreased by a factor of 1.9 to account for the mean bias relative to the OMI-derived product. This shows that the geographical patterns are consistent between the two data sets, with correlation coefficient r = 0.59 in the East (>−95° longitude) and r = 0.56 in the West. The factor of 1.9 bias will be used in the section below as representing the range of uncertainty in annual mean HCHO concentrations.

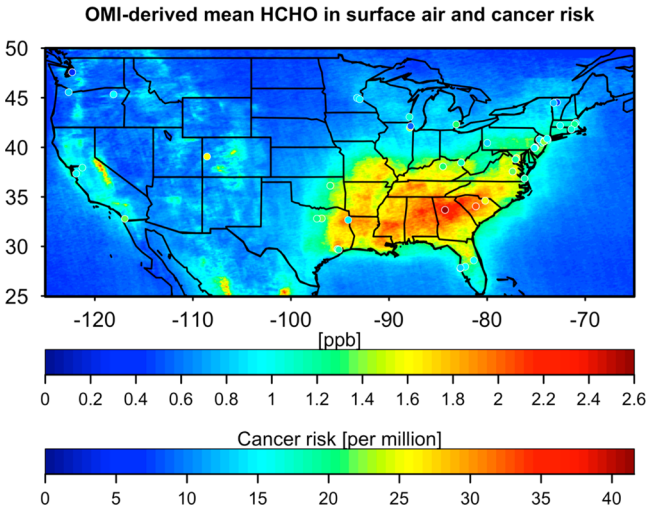

Figure 7. OMI-derived annual mean HCHO concentrations in surface air and associated cancer risks. Cancer risk is related to surface HCHO concentration using the upper-bound EPA inhalation unit risk estimate (URE) of 1.3 × 10^{-5} (μg m^{-3})$^{-1}$. The EPA SLTs network data of Figure 1 are superimposed as circles, decreased by a factor of 1.9 to account for the mean bias relative to the OMI-derived data (see text).

National Cancer Risks from Outdoor HCHO Exposure. Figure 7 shows the distribution of cancer risks in the U.S. inferred from the OMI-derived mean surface HCHO concentrations, based on the EPA URE given as an upper bound and a conversion factor of 1.23 μg m^{-3} ppb^{-1} at 298 K and 1 atm. We estimate the total national cancer risk from HCHO exposure by convolving the OMI-derived distribution of cancer risks in Figure 7 with gridded 0.05° × 0.05° population data for 2015.[49] We infer in this manner that up to 6600 people in the U.S. will develop cancer at some point in their lives due to exposure to outdoor HCHO. If annual mean HCHO concentrations are scaled up by 1.9 to match the EPA SLTs data then the upper bound for the number of cancer rates correspondingly increases. Thus, the upper bound for lifelong cancer occurrences due to exposure to outdoor HCHO over the U.S. is in the range 6600−12500, *i.e.*, one person in 25 500−48 300 from a U.S. population of 319 million. This cancer risk is well above the 1 in 10^6 level generally considered as the threshold of tolerable risk.[50,51] Based on a U.S. life expectancy of 78.7 years (2012), it translates into 84−160 cancer cases per year in the U.S. caused by exposure to outdoor HCHO.

Co-Benefit of NO_x Emission Controls for Reducing HCHO-Related Cancer Risks. HCHO in the U.S. originates mostly from the oxidation of biogenic isoprene emitted by vegetation, and thus would seem largely uncontrollable. However, the HCHO yield from isoprene oxidation is higher in the presence of nitrogen oxide radicals ($NO_x \equiv NO + NO_2$)[52,53] and NO_x in the U.S. is mainly anthropogenic. The dependence of the HCHO yield on NO_x levels is nonlinear,[45,53] and there is uncertainty regarding current U.S. NO_x emissions,[54] thus any quantitative policy-relevant estimate based on incremental decrease in NO_x emission would be very uncertain. We conducted a sensitivity GEOS-Chem simulation with no anthropogenic NO_x emissions and found that HCHO annual mean surface concentrations in the U.S. decrease by 10−30% depending on location. Convolving this decrease with the U.S. population map, we find that cancer risks from outdoor HCHO decrease by 20%. Thus, the increment in HCHO cancer risks due to anthropogenic NO_x is 4.1−7.8 person in 10^6, which by itself is above the tolerable threshold of 1 in 10^6. Anthropogenic NO_x emissions in the U.S. have decreased by 2.1% a^{-1} over 1991−2013 in response to regulations to improve ozone air quality and attain NO_2 air quality standards.[55] Such efforts to mitigate NO_x emissions thus have a significant cobenefit in also reducing HCHO-related cancer risks.

AUTHOR INFORMATION

Corresponding Author

*E-mail: leizhu@fas.harvard.edu.

ORCID

Lei Zhu: 0000-0002-3919-3095

Viral Shah: 0000-0001-5547-106X

Present Address

¶(M.B.) Utah Department of Environmental Quality, Salt Lake City, Utah, United States.

Notes

The authors declare no competing financial interest.

DOI: 10.1021/acs.est.7b01356
Environ. Sci. Technol. XXXX, XXX, XXX−XXX

■ ACKNOWLEDGMENTS

This work was supported by the NASA Earth Science Division. Funding for the SLAQRS measurements was provided by NSF (Grant #1148951). We thank Noelle Selin for valuable discussions on HCHO cancer risks.

■ REFERENCES

(1) *Technical Support Document EPA's 2011 National-scale Air Toxics Assessment, 2011 NATA TSD*; United States Environmental Protection Agency: United States, 2015; https://www.epa.gov/sites/production/files/2015-12/documents/2011-nata-tsd.pdf (accessed on April 17, 2017).

(2) Strum, M.; Scheffe, R. National review of ambient air toxics observations. *J. Air Waste Manage. Assoc.* **2016**, *66* (2), 120−133.

(3) Palmer, P. I.; Jacob, D. J.; Fiore, A. M.; Martin, R. V.; Chance, K.; Kurosu, T. P. Mapping isoprene emissions over North America using formaldehyde column observations from space. *J. Geophys. Res.* **2003**, *108* (D6), 4180.

(4) González Abad, G.; Liu, X.; Chance, K.; Wang, H.; Kurosu, T. P.; Suleiman, R. Updated Smithsonian Astrophysical Observatory Ozone Monitoring Instrument (SAO OMI) formaldehyde retrieval. *Atmos. Meas. Tech.* **2015**, *8* (1), 19−32.

(5) Zhu, L.; Jacob, D. J.; Mickley, L. J.; Marais, E. A.; Cohan, D. S.; Yoshida, Y.; Duncan, B. N.; González Abad, G.; Chance, K. V. Anthropogenic emissions of highly reactive volatile organic compounds in eastern Texas inferred from oversampling of satellite (OMI) measurements of HCHO columns. *Environ. Res. Lett.* **2014**, *9* (11), 114004.

(6) *Compendium Method TO-11A Determination of Formaldehyde in Ambient Air Using Adsorbent Cartridge Followed by High Performance Liquid Chromatography (HPLC) [Active Sampling Methodology]*; United States Environmental Protection Agency: United States, 1999; https://www3.epa.gov/ttnamti1/files/ambient/airtox/to-11ar.pdf (accessed on April 17, 2017).

(7) Achatz, S.; Lörinci, G.; Hertkorn, N.; Gebefügi, I.; Kettrup, A. Disturbance of the determination of aldehydes and ketones: structural elucidation of degradation products derived from the reaction of 2,4-Dinitrophenylhydrazine (DNPH) with ozone. *Fresenius' J. Anal. Chem.* **1999**, *364* (1), 141−146.

(8) Karst, U.; Binding, N.; Cammann, K.; Witting, U. Interferences of nitrogen dioxide in the determination of aldehydes and ketones by sampling on 2,4-dinitrophenylhydrazine-coated solid sorbent. *Fresenius' J. Anal. Chem.* **1993**, *345* (1), 48−52.

(9) Tang, S.; Graham, L.; Shen, L.; Zhou, X.; Lanni, T. Simultaneous determination of carbonyls and NO_2 in exhausts of heavy-duty diesel trucks and transit buses by HPLC following 2,4-dinitrophenylhydrazine cartridge collection. *Environ. Sci. Technol.* **2004**, *38* (22), 5968−5976.

(10) Ryerson, T. B.; Andrews, A. E.; Angevine, W. M.; Bates, T. S.; Brock, C. A.; Cairns, B.; Cohen, R. C.; Cooper, O. R.; de Gouw, J. A.; Fehsenfeld, F. C.; Ferrare, R. A.; Fischer, M. L.; Flagan, R. C.; Goldstein, A. H.; Hair, J. W.; Hardesty, R. M.; Hostetler, C. A.; Jimenez, J. L.; Langford, A. O.; McCauley, E.; McKeen, S. A.; Molina, L. T.; Nenes, A.; Oltmans, S. J.; Parrish, D. D.; Pederson, J. R.; Pierce, R. B.; Prather, K.; Quinn, P. K.; Seinfeld, J. H.; Senff, C. J.; Sorooshian, A.; Stutz, J.; Surratt, J. D.; Trainer, M.; Volkamer, R.; Williams, E. J.; Wofsy, S. C. The 2010 California Research at the Nexus of Air Quality and Climate Change (CalNex) Field Study. *J. Geophys. Res.* **2013**, *118* (11), 5830−5866.

(11) Lin, Y. C.; Schwab, J. J.; Demerjian, K. L.; Bae, M.-S.; Chen, W.-N.; Sun, Y.; Zhang, Q.; Hung, H.-M.; Perry, J. Summertime formaldehyde observations in New York City: Ambient levels, sources and its contribution to HOx radicals. *J. Geophys. Res.* **2012**, *117* (D8), D08305.

(12) Millet, D. B.; Baasandorj, M.; Hu, L.; Mitroo, D.; Turner, J.; Williams, B. J. Nighttime chemistry and morning isoprene can drive daytime ozone downwind of a major deciduous forest. *Environ. Sci. Technol.* **2016**, *50* (8), 4335−4342.

(13) Sareen, N.; Carlton, A. G.; Surratt, J. D.; Gold, A.; Lee, B.; Lopez-Hilfiker, F. D.; Mohr, C.; Thornton, J. A.; Zhang, Z.; Lim, Y. B.; Turpin, B. J. Identifying precursors and aqueous organic aerosol formation pathways during the SOAS campaign. *Atmos. Chem. Phys.* **2016**, *16* (22), 14409−14420.

(14) Zhu, L.; Jacob, D. J.; Kim, P. S.; Fisher, J. A.; Yu, K.; Travis, K. R.; Mickley, L. J.; Yantosca, R. M.; Sulprizio, M. P.; De Smedt, I.; Gonzalez Abad, G.; Chance, K.; Li, C.; Ferrare, R.; Fried, A.; Hair, J. W.; Hanisco, T. F.; Richter, D.; Scarino, A. J.; Walega, J.; Weibring, P.; Wolfe, G. M. Observing atmospheric formaldehyde (HCHO) from space: validation and intercomparison of six retrievals from four satellites (OMI, GOME2A, GOME2B, OMPS) with SEAC^{4}RS aircraft observations over the Southeast US. *Atmos. Chem. Phys.* **2016**, *16* (21), 13477−13490.

(15) Martin, R. V.; Parrish, D. D.; Ryerson, T. B.; Nicks, D. K., Jr.; Chance, K.; Kurosu, T. P.; Jacob, D. J.; Sturges, E. D.; Fried, A.; Wert, B. P. Evaluation of GOME satellite measurements of tropospheric NO_2 and HCHO using regional data from aircraft campaigns in the southeastern United States. *J. Geophys. Res.* **2004**, *109* (D24), D24307.

(16) Millet, D. B.; Jacob, D. J.; Turquety, S.; Hudman, R. C.; Wu, S.; Fried, A.; Walega, J.; Heikes, B. G.; Blake, D. R.; Singh, H. B.; Anderson, B. E.; Clarke, A. D. Formaldehyde distribution over North America: Implications for satellite retrievals of formaldehyde columns and isoprene emission. *J. Geophys. Res.* **2006**, *111* (D24), D24S02.

(17) Chance, K.; Palmer, P. I.; Spurr, R. J. D.; Martin, R. V.; Kurosu, T. P.; Jacob, D. J. Satellite observations of formaldehyde over North America from GOME. *Geophys. Res. Lett.* **2000**, *27* (21), 3461−3464.

(18) Wittrock, F.; Richter, A.; Oetjen, H.; Burrows, J. P.; Kanakidou, M.; Myriokefalitakis, S.; Volkamer, R.; Beirle, S.; Platt, U.; Wagner, T. Simultaneous global observations of glyoxal and formaldehyde from space. *Geophys. Res. Lett.* **2006**, *33* (16), L16804.

(19) De Smedt, I.; Stavrakou, T.; Hendrick, F.; Danckaert, T.; Vlemmix, T.; Pinardi, G.; Theys, N.; Lerot, C.; Gielen, C.; Vigouroux, C.; Hermans, C.; Fayt, C.; Veefkind, P.; Müller, J.-F.; Van Roozendael, M. Diurnal, seasonal and long term variations of global formaldehyde columns inferred from combined OMI and GOME-2 observations. *Atmos. Chem. Phys.* **2015**, *15* (21), 12519−12545.

(20) De Smedt, I.; Van Roozendael, M.; Stavrakou, T.; Müller, J.-F.; Lerot, C.; Theys, N.; Valks, P.; Hao, N.; van der A, R. Improved retrieval of global tropospheric formaldehyde columns from GOME-2/MetOp-A addressing noise reduction and instrumental degradation issues. *Atmos. Meas. Tech.* **2012**, *5* (11), 2933−2949.

(21) Li, C.; Joiner, J.; Krotkov, N. A.; Dunlap, L. A new method for global retrievals of HCHO total columns from the Suomi National Polar-orbiting Partnership Ozone Mapping and Profiler Suite. *Geophys. Res. Lett.* **2015**, *42* (7), 2515−2522.

(22) González Abad, G.; Vasilkov, A.; Seftor, C.; Liu, X.; Chance, K. Smithsonian Astrophysical Observatory Ozone Mapping and Profiler Suite (SAO OMPS) formaldehyde retrieval. *Atmos. Meas. Tech.* **2016**, *9* (7), 2797−2812.

(23) Abbot, D. S.; Palmer, P. I.; Martin, R. V.; Chance, K. V.; Jacob, D. J.; Guenther, A. Seasonal and interannual variability of North American isoprene emissions as determined by formaldehyde column measurements from space. *Geophys. Res. Lett.* **2003**, *30* (17), 1886.

(24) Levelt, P. F.; van den Oord, G. H. J.; Dobber, M. R.; Malkki, A.; Visser, H.; de Vries, J.; Stammes, P.; Lundell, J. O. V.; Saari, H. The Ozone monitoring instrument. *IEEE Trans. Geo. Rem. Sens.* **2006**, *44* (5), 1093−1101.

(25) De Smedt, I.; Müller, J.-F.; Stavrakou, T.; van der A, R.; Eskes, H.; Van Roozendael, M. Twelve years of global observations of formaldehyde in the troposphere using GOME and SCIAMACHY sensors. *Atmos. Chem. Phys.* **2008**, *8* (16), 4947−4963.

(26) Boeke, N. L.; Marshall, J. D.; Alvarez, S.; Chance, K. V.; Fried, A.; Kurosu, T. P.; Rappenglück, B.; Richter, D.; Walega, J.; Weibring, P.; Millet, D. B. Formaldehyde columns from the Ozone Monitoring Instrument: Urban versus background levels and evaluation using aircraft data and a global model. *J. Geophys. Res.* **2011**, *116* (D5), D05303.

DOI: 10.1021/acs.est.7b01356
Environ. Sci. Technol. XXXX, XXX, XXX−XXX

(27) Toon, O. B.; Maring, H.; Dibb, J.; Ferrare, R.; Jacob, D. J.; Jensen, E. J.; Luo, Z. J.; Mace, G. G.; Pan, L. L.; Pfister, L.; Rosenlof, K. H.; Redemann, J.; Reid, J. S.; Singh, H. B.; Thompson, A. M.; Yokelson, R.; Minnis, P.; Chen, G.; Jucks, K. W.; Pszenny, A. Planning, implementation, and scientific goals of the Studies of Emissions and Atmospheric Composition, Clouds and Climate Coupling by Regional Surveys (SEAC^{4}RS) field mission. *J. Geophys. Res. Atmos.* **2016**, *121* (9), 4967−5009.
(28) Richter, D.; Weibring, P.; Walega, J. G.; Fried, A.; Spuler, S. M.; Taubman, M. S. Compact highly sensitive multi-species airborne mid-IR spectrometer. *Appl. Phys. B: Lasers Opt.* **2015**, *119* (1), 119−131.
(29) Cazorla, M.; Wolfe, G. M.; Bailey, S. A.; Swanson, A. K.; Arkinson, H. L.; Hanisco, T. F. A new airborne laser-induced fluorescence instrument for in situ detection of formaldehyde throughout the troposphere and lower stratosphere. *Atmos. Meas. Tech.* **2015**, *8* (2), 541−552.
(30) Anderson, D.; Nicely, J.; Salawitch, R.; Wolfe, G.; Hanisco, T.; Dickerson, R.; Canty, T.; Li, C.; *Evaluation of Satellite HCHO Retrievals over the Tropical Western Pacific and United States*, AGU Fall Meeting, San Francisco, United States, December 12−16, 2016.
(31) González Abad, G.; Liu, X.; Chance, K.; Fried, A.; Irie, H.; *Validation of the new SAO OMI formaldehyde retrievals*, AGU Fall Meeting, San Francisco, United States, December 15−19, 2014.
(32) Streets, D.; Canty, T.; Carmichael, G.; de Foy, B.; Dickerson, R.; Duncan, B.; Edwards, D.; Haynes, J.; Henze, D.; Houyoux, M.; Jacob, D.; Krotkov, N.; Lamsal, L.; Liu, Y.; Lu, Z.; Martin, R.; Pfister, G. G.; Pinder, R. W.; Salawitch, R. J.; Wecht, K. Emissions estimation from satellite retrievals: A review of current capability. *Atmos. Environ.* **2013**, *77*, 1011−1042.
(33) McLinden, C. A.; Fioletov, V.; Boersma, K. F.; Krotkov, N.; Sioris, C. E.; Veefkind, J. P.; Yang, K. Air quality over the Canadian oil sands: A first assessment using satellite observations. *Geophys. Res. Lett.* **2012**, *39* (4), L04804.
(34) de Foy, B.; Krotkov, N.; Bei, N.; Herndon, S.; Huey, L.; Martínez, A.-P.; Ruiz-Su_arez, L.; Wood, E.; Zavala, M.; Molina, L. Hit from both sides: tracking industrial and volcanic plumes in Mexico City with surface measurements and OMI SO_2 retrievals during the MILAGRO field campaign. *Atmos. Chem. Phys.* **2009**, *9* (24), 9599−9617.
(35) Fioletov, V. E.; McLinden, C. A.; Krotkov, N.; Moran, M. D.; Yang, K. Estimation of SO_2 emissions using OMI retrievals. *Geophys. Res. Lett.* **2011**, *38* (21), L21811.
(36) Lu, Z.; Streets, D. G.; de Foy, B.; Krotkov, N. A. Ozone Monitoring Instrument observations of interannual increases in SO_2 emissions from Indian coal-fired power plants during 2005−2012. *Environ. Sci. Technol.* **2013**, *47* (24), 13993−14000.
(37) De Graaf, M.; Sihler, H.; Tilstra, L. G.; Stammes, P. How big is an OMI pixel? *Atmos. Meas. Tech.* **2016**, *9* (8), 3607−3618.
(38) Millet, D. B.; Jacob, D. J.; Boersma, K. F.; Fu, T. M.; Kurosu, T. P.; Chance, K.; Heald, C. L.; Guenther, A. Spatial distribution of isoprene emissions from North America derived from formaldehyde column measurements by the OMI satellite sensor. *J. Geophys. Res.* **2008**, *113* (D2), D02307.
(39) Rappenglück, B.; Dasgupta, P. K.; Leuchner, M.; Li, Q.; Luke, W. Formaldehyde and its relation to CO, PAN, and SO_2 in the Houston-Galveston airshed. *Atmos. Chem. Phys.* **2010**, *10* (5), 2413−2424.
(40) Rappenglück, B.; Lubertino, G.; Alvarez, S.; Golovko, J.; Czader, B.; Ackermann, L. Radical Precursors and Related Species from Traffic as Observed and Modeled at an Urban Highway Junction. *J. Air Waste Manage. Assoc.* **2013**, *63* (11), 1270−1286.
(41) Johansson, J. K. E.; Mellqvist, J.; Samuelsson, J.; Offerle, B.; Moldanova, J.; Rappenglück, B.; Lefer, B.; Flynn, J. Quantitative measurements and modeling of industrial formaldehyde emissions in the Greater Houston area during campaigns in 2009 and 2011. *J. Geophys. Res. Atmos.* **2014**, *119* (7), 4303−4322.
(42) Fu, T.-M.; Jacob, D. J.; Palmer, P. I.; Chance, K.; Wang, Y. X.; Barletta, B.; Blake, D. R.; Stanton, J. C.; Pilling, M. J. Space-based formaldehyde measurements as constraints on volatile organic compound emissions in east and south Asia and implications for ozone. *J. Geophys. Res.* **2007**, *112* (D6), D06312.
(43) Molod, A.; Takacs, L.; Suarez, M.; Bacmeister, J.; Song, I.-S.; Eichmann, A. The GEOS-5 Atmospheric General Circulation Model: Mean Climate and Development from MERRA to Fortuna. NASA/TM−2012, 2012, *28*, 104606.
(44) Palmer, P. I.; Abbot, D. S.; Fu, T.-M.; Jacob, D. J.; Chance, K.; Kurosu, T. P.; Guenther, A.; Wiedinmyer, C.; Stanton, J. C.; Pilling, M. J.; Pressley, S. N.; Lamb, B.; Sumner, A. L. Quantifying the seasonal and interannual variability of North American isoprene emissions using satellite observations of the formaldehyde column. *J. Geophys. Res.* **2006**, *111* (D12), D12315.
(45) Chan Miller, C.; Jacob, D. J.; Marais, E. A.; Yu, K.; Travis, K. R.; Kim, P. S.; Fisher, J. A.; Zhu, L.; Wolfe, G. M.; Keutsch, F. N.; Kaiser, J.; Min, K.-E.; Brown, S. S.; Washenfelder, R. A.; González Abad, G.; Chance, K. Glyoxal yield from isoprene oxidation and relation to formaldehyde: chemical mechanism, constraints from SENEX aircraft observations, and interpretation of OMI satellite data. *Atmos. Chem. Phys. Discuss.* **2016**, 1.
(46) Jaeglé, L.; Thornton, J. A.; Brown, S. S.; Shah, V.; Lopez-Hilfiker, F.; Lee, B. H.; Haskins, J.; Fibiger, D. L.; McDuffie, E. E.; Sparks, T.; Ebben, C. J.; Wooldridge, P. J.; Cohen, R. C.; Veres, P. R.; Weinheimer, A. J.; Montzka, D. D.; Dibb, J. E.; Schroder, J. C.; Jost, P. C.; Day, D. A.; Jimenez, J. L.; Sullivan, A.; Guo, H.; Weber, R. J.; Green, J. R.; Fiddler, M. N.; Bililign, S.; Campos, T. L.; Apel, J. R.; Blake, N. J.; Hall, S. R.; Ullmann, K.; Wolfe, G. M.; DiGangi, J. P.; Hanisco, T. F.; Leen, J. B. *Sources, Chemistry, and Transport of Pollutants over the Eastern United States During the WINTER 2015 Aircraft Campaign*, AGU Fall Meeting, San Francisco, United States, December 14−18, 2015.
(47) Dasgupta, P. K.; Li, J.; Zhang, G.; Luke, W. T.; McClenny, W. A.; Stutz, J.; Fried, A. Summertime ambient formaldehyde in five U.S. metropolitan areas: Nashville, Atlanta, Houston, Philadelphia, and Tampa. *Environ. Sci. Technol.* **2005**, *39* (13), 4767−4783.
(48) Sumner, A. L.; Shepson, P. B.; Couch, T. L.; Thornberry, T.; Carroll, M. A.; Sillman, S.; Pippin, M.; Bertman, S.; Tan, D.; Faloona, I.; Brune, W.; Young, V.; Cooper, O.; Moody, J.; Stockwell, W. A study of formaldehyde chemistry above a forest canopy. *J. Geophys. Res.* **2001**, *106* (D20), 24387−24405.
(49) Gridded Population of the World, Version 3 (GPWv3): Population Density Grid, Future Estimates; http://dx.doi.org/10.7927/H4ST7MRB (accessed on April 17, 2017).
(50) *Water Quality Standards Handbook, Chapter 3: Water Quality Criteria*; United States Environmental Protection Agency: United States, 1994; https://www.epa.gov/sites/production/files/2014-10/documents/handbook-Chapter3.pdf (accessed on April 17, 2017).
(51) *Guidance on Information Requirements and Chemical Safety Assessment, Chapter R.8: Characterisation of Dose [Concentration]-Response for Human Health*; European Chemicals Agency: Helsinki, Finland, 2012; https://echa.europa.eu/documents/10162/13632/information_requirements_r8_en.pdf (accessed on April 17, 2017).
(52) Marais, E. A.; Jacob, D. J.; Kurosu, T. P.; Chance, K.; Murphy, J. G.; Reeves, C.; Mills, G.; Casadio, S.; Millet, D. B.; Barkley, M. P.; Paulot, F.; Mao, J. Isoprene emissions in Africa inferred from OMI observations of formaldehyde columns. *Atmos. Chem. Phys.* **2012**, *12* (14), 6219−6235.
(53) Wolfe, G. M.; Kaiser, J.; Hanisco, T. F.; Keutsch, F. N.; de Gouw, J. A.; Gilman, J. B.; Graus, M.; Hatch, C. D.; Holloway, J.; Horowitz, L. W.; Lee, B. H.; Lerner, B. M.; Lopez-Hilifiker, F.; Mao, J.; Marvin, M. R.; Peischl, J.; Pollack, I. B.; Roberts, J. M.; Ryerson, T. B.; Thornton, J. A.; Veres, P. R.; Warneke, C. Formaldehyde production from isoprene oxidation across NO_x regimes. *Atmos. Chem. Phys.* **2016**, *16* (4), 2597−2610.
(54) Travis, K. R.; Jacob, D. J.; Fisher, J. A.; Kim, P. S.; Marais, E. A.; Zhu, L.; Yu, K.; Miller, C. C.; Yantosca, R. M.; Sulprizio, M. P.; Thompson, A. M.; Wennberg, P. O.; Crounse, J. D.; St. Clair, J. M.; Cohen, R. C.; Laughner, J. L.; Dibb, J. E.; Hall, S. R.; Ullmann, K.; Wolfe, G. M.; Pollack, I. B.; Peischl, J.; Neuman, J. A.; Zhou, X. Why

DOI: 10.1021/acs.est.7b01356
Environ. Sci. Technol. XXXX, XXX, XXX−XXX

do models overestimate surface ozone in the Southeast United States? *Atmos. Chem. Phys.* **2016**, *16* (21), 13561−13577.
(55) *Air Pollutant Emissions Trends Data: Average Annual Emissions*; United States Environmental Protection Agency: United States, 2015; https://www.epa.gov/air-emissions-inventories/air-pollutant-emissions-trends-data (accessed on April 17, 2017).

DOI: 10.1021/acs.est.7b01356
Environ. Sci. Technol. XXXX, XXX, XXX−XXX